2020-01-1606 Published 05 Oct 2020



# A Coupling Analysis of Thermal Buckling and Vibration in Disc Brakes

Joseph-shaahu Shaahu, Kingsford Koranteng, and Yun-Bo Yi University of Denver

Citation: Shaahu, J.-S., Koranteng, K., and Yi, Y.-B., "A Coupling Analysis of Thermal Buckling and Vibration in Disc Brakes," SAE Technical Paper 2020-01-1606, 2020, doi:10.4271/2020-01-1606.

#### **Abstract**

non-uniform high-temperature gradient is generated on the surface of brake disc during braking. This temperature gradient induces thermal buckling, a deformation characterized by either a coning mode or potato chip mode. In rotating machinery, vibration occurs with a natural frequency at a certain rotational speed, leading to a change in the contact conditions at the frictional interface. It may cause a redistribution of temperature and thus the thermal buckling modes. Meanwhile, some vibration modes in a brake system can also be excited by the deformation modes of thermal buckling in the rotor. The coupled and uncoupled problems of thermal buckling and vibration are analyzed using an ABAQUS benchmark vented brake model. It is known that

different assumptions of temperature, either in the radial or axial direction, may lead to different solutions of thermal buckling. In this study, we assumed some representative temperature profiles in the radial direction, including linear, sinusoidal, and exponential functions, meanwhile, the circumferential distribution of temperature was maintained uniform. The effect of structural vibration on the thermal buckling modes, as well as the effect of buckling modes on vibration in this simplified situation, were both analyzed. Although it is concluded that vibration during braking does not significantly increase the chance of buckling for the ABAQUS benchmark model, the results are highly dependent on the chosen parameters including materials, dimensions, and rotational velocity, and the coupling can be strong in some conditions.

## Introduction

ibrations have been used to study the equilibrium state of a system. Such simplified systems are often represented with a mass and spring system. Although it would be reasonable to assume a vibrating system is out of balance, the amplitude of a frequency determines the severity of a fault [1]. In reality, vibrating systems or bodies are not necessarily out of balance. Every body vibrates at a certain frequency; this frequency is known as the natural frequency of the body. Various studies of vibration have been conducted throughout the years in various areas, such as human anatomy, civil and structural engineering, mechanics, automotive industry, etc. Most vibration studies conducted for the automotive industry have been on the brake disc and these have mainly been squeal analysis and brake judder analysis. Brake judder is a braking induced forced vibration occurring in different types of vehicles. Brake judder is usually felt in the steering wheel, which affects the operation of the vehicle and can cause veering. Hence, the study of such has been prudent so as to reduce the transfer frequency from the brake to the steering wheel. The first two modes of the wheel are the dominant vibration modes and the vibration signal of the brake pedal has similar components to the steering wheel, except for showing lower vibration amplitudes in the natural frequencies of the transfer path [2]. Meyer, Ralf [3] studied

disc brake judder that is attributable to thickness variations in the disc and that these deviations from the ideal plane surface can be caused either by wear and corrosion or by thermal stresses (changes within the microstructure of the disc material). They are termed "cold judder" and "thermal judder" respectively.

It is known that automotive brakes and clutches can fail at elevated temperatures and thermal stresses due to the frictional heat generation at the contact surfaces during brake operations or clutch engagements. The mechanism of failure, however, varies depending on the operating conditions. Thermal buckling is believed to be one of the dominant failure mechanisms in clutch plates due to their small thicknesses [4]. It cannot be said the same for brake rotors due to its slightly bigger thickness and non-axisymmetrical geometry. Stibich, Paul R., et al. developed a technique to predict thermal buckling by obtaining temperature profiles from a heat transfer analysis and applied in the buckling analysis [5].

Audebert et al. studies on buckling of automotive clutch plates due to thermoelastic residual stresses revealed that clutch plates subjected to axisymmetric temperature excursions can develop residual in-plane bending moments of sufficient magnitude to cause buckling during unloading. The coning mode occurred when the residual stress at the outer radius was tensile and the potato chip mode occurred when

it was compressive [6]. Ma extended the method to automotive disc brakes and investigated the effect of geometric and material parameters on the critical buckling loads via the finite element method. These studies revealed that both axisymmetric and non-axisymmetric buckling modes can be caused by a uniformly distributed thermal loading in the circumferential direction [7]. In addition, a slightly changed temperature profile in the radial direction can greatly affect the buckling modes.

In previous investigations of thermal buckling, a simplified geometry of an annular ring was used and assumed a hundred percent contact area at the frictional interface during braking. However, if there is some vibrational deflection, the contact area at the frictional interface will be affected by the vibrational distortion which can affect the distribution of the temperature generated during braking. Therefore, it is essential to study the coupling between vibration and thermal buckling. The present work will investigate the coupling of vibration and thermal buckling in brakes by taking into account various vehicle speeds that affect the vibration modes and investigate if vibration does increase the possibility of thermal buckling. It should also be noted that vibration modes can also be excited by the thermal buckling modes. Palmer, E, et al. stated that in high-demand braking applications, vented discs are increasingly being used as these are considered to have high heat-dissipating characteristics [8]. Therefore, a more realistic vented brake model will be analyzed in this study. Based on previous works, finite element analysis has proven to be efficient in analyzing vibrations and thermal buckling. Therefore, a finite element method is chosen for the coupling numerical study of vibration and thermal buckling in automotive brake discs.

## **Method**

The geometric model of the brake rotor is based on the benchmark brake model for squeal analysis in ABAQUS [9]. Cast irons are commonly used in brake discs production because of low costs of production, the excellent thermal conductivity, the ease of dissipating heat generated by the friction of the pads during a stop, and the capacity of damping vibrations, which are prime characteristics of this kind of component [10]. Therefore, cast iron was the chosen material in this study for the brake rotor. The meshed 3D model is a mixture of 8-noded hex element (C3D8) and wedge elements (C3D6) with 25,457 nodes and 17,105 elements. Figure 1 shows the brake rotor in the meshed state before the analysis is conducted. Table 1 shows the dimensions of the brake rotor and Table 2 shows the material properties for gray cast iron. Figure 2 shows a cross-section schematic of the brake rotor to illustrate the dimensions shown in Table 1. The setup for the study only required some constraints to be placed on the model. The constraints on the model followed a realistic boundary condition for a brake rotor, where the brake rotor is fixed to the wheel of the car via the bolts, and the inner and outer radii are free. The same constraints were used in both the vibration and thermal buckling simulations. Initial conditions were imposed on the brake rotor for both the vibration and thermal

**FIGURE 1** Finite element model of a brake disc. It is based on the brake squeal analysis benchmark model in ABAQUS [9]

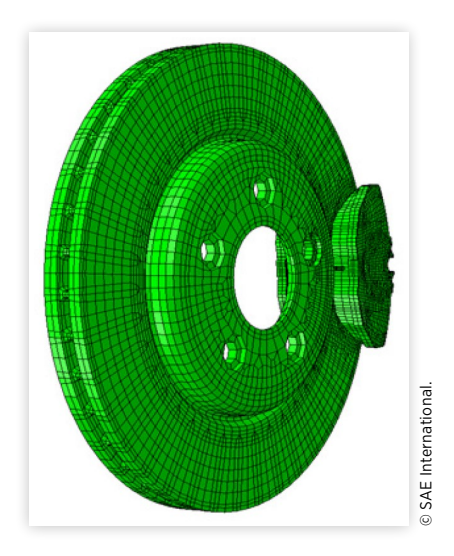
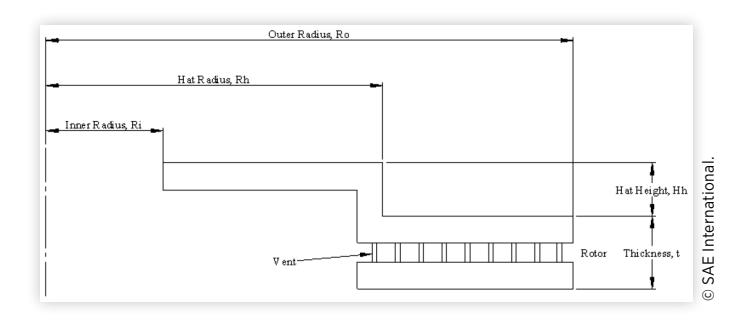


**TABLE 1** Geometric dimensions of the brake rotor

	Outer Radius	Inner Radius	Hat Radius	Hat Height	Thickness
Symbol	Ro	Ri	Rh	Hh	t
Unit	mm	mm	mm	mm	mm
Value	144	32	92	13	20

© SAE International.

**FIGURE 2** A cross-section schematic of the brake rotor used in this study



buckling studies. The applied initial conditions for the vibration and thermal buckling simulations are rotational velocity in rad/s and prescribed temperature field in degree Celsius respectively. Highway speed, interstate speed, and school zone speed limits were used in the vibration study and converted to rotational velocity using <u>Equation 2</u>.

Various temperature profiles are used in the thermal buckling analysis. Linear, exponential and sinusoidal distributions have been found among the most representative temperature profiles. The linear distribution can be caused by the sliding speed as a linear function of the radius and by the fact that the frictional heat generation rate is a linear function of the sliding speed. The sinusoidal distribution is related to the local high-temperature regions known as hot spots that could be excited by thermoelastic instability. An exponential distribution can

**TABLE 2** Material properties of the brake rotor

	Young's Modulus	Mass Density	Poisson's Ratio	Thermal Expansion	Thermal Conductivity	Specific Heat
Symbol	Е	ρ	ν	α	k	Ср
Unit	MPa	Kg/m <sup>3</sup>	NA	10 <sup>-5</sup> /K	W/m*K	J/kg*K
Value	66178.1	7200	0.27	1.2	45	510

be caused by the non-uniform convective cooling on the surface or a non-uniform contact pressure during the engagement and separation of plates and similarly the engagement and separation of the rotor and brake pads. For reasons stated earlier, a linear, sinusoidal and exponential temperature profiles are used in the buckling simulation. In this study, a maximum temperature of 250°C was assumed for all buckling simulation to correspond with Belhocine Ali, and Mostefa Bouchetara's [11] finding of average temperatures through a disc thickness of three types of cast irons. For the purpose of this paper, it is also assumed that displacement is proportional to temperature as shown in Equation 1 so as to perform the coupling analysis. The coupling study consists of four consecutive steps. The first step includes the conducted vibration simulation and exporting the resulting displacement from the simulation into excel. The second step is calculating the k value and generating a nodal temperature data. The k value is calculated using the maximum displacement obtained from step 1 and calculated to have the node with the corresponding maximum displacement have a maximum temperature of 250°C. The value of k is then multiplied by the displacement results obtained in step 1 to generate a dataset of nodal temperatures. Thirdly, a plot of temperature as a function of the nodes radial and axial locations is created and a regression toolbox is utilized to fit an equation to the curve that best describes the plot. Lastly, the equation obtained in the third step is used to describe the prescribed temperature field varying in the radial or axial direction for the thermal buckling simulation. All loading and constraint conditions applied follows a cylindrical axis system radial (R), circumferential (theta,  $\theta$ ), and axial (z).

$$U\alpha \frac{1}{k} \times T \tag{1}$$

## **Results and Discussions**

## Effect of Rotational Speeds on Vibration

The rotational velocity was calculated using <u>Equation 2</u>, assuming a traveling speed of the vehicle in miles per hour (mph). The speed of the vehicle in miles per hour (mph) is then converted to meters per hour and then to meters per minute. Using the circumference of the wheel in meters, convert meters per minute to revolutions per minute (rpm), which is then converted to rotational velocity in radians per second (rad/s).

$$RV = S_v \times \left(\frac{1609.34}{3600 \times R}\right)$$
 (2)

Here, RV represents rotational velocity in radians per second,  $S_v$  represents the speed of the vehicle in miles per hour

and R represents the radius of the wheel in meters, not to be confused with the radius of the brake rotor. The radius of the wheel used in this study is based on Daws, J. W., et al. [12] Chevrolet Avalanche wheel radius of 0.389m. Using Equation 1, the calculated rotational velocities from speeds of 25mph, 55mph, and 75mph are 29rad/s, 63rad/s, and 86rad/s respectively. Table 3 shows the result obtained from the vibrational study with the calculated rotational velocities. It should be noted the displacement in Table 3 is the resultant displacement. As seen in Table 3, the displacement and damped frequency got lower at higher speeds.

The corresponding vibration mode with a rotational speed of 86rad/s is shown in <u>Figure 3</u>. <u>Figure 3</u> also shows an out-of-plane vibration mode with one node diameter. The color represents the values of the resultant displacement, where red and blue corresponds to the maximum and minimum value respectively.

A path parallel to the global y-axis was created on the brake disc midplane to describe the brake discs' radial location. Another path parallel to the global z-axis was created on the brake disc top plane to describe the brake discs' axial location. Figures 4 and 5 are plots of displacement as a function of the brake discs' radial location and axial location respectively at 86rad/s. The zero values shown in Figure 4 represent the vent space and the hollow area of the rotor hat, while the zero values in Figure 5 represent the empty area of the inner radius. The x-axis in Figures 4, 5, 9, and 10

**TABLE 3** Vibration study results

<del>_</del>	Element Type		C3D8 & C3D6		
tional.	Rotational Velocity [rad/s]		29	63	86
Interna	Damped Frequency [Hz]		674.11	670.55	667.65
SAEInt	Displacement [mm] Maximum		26.694	24.745	23.817
⊗ S/		Minimum	0	0	0

FIGURE 3 Mode 1 axially deformed result at 86rad/s of the brake rotor

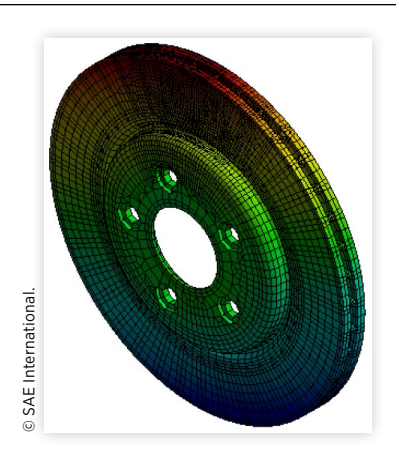


FIGURE 4 Resultant displacement vs. axial location

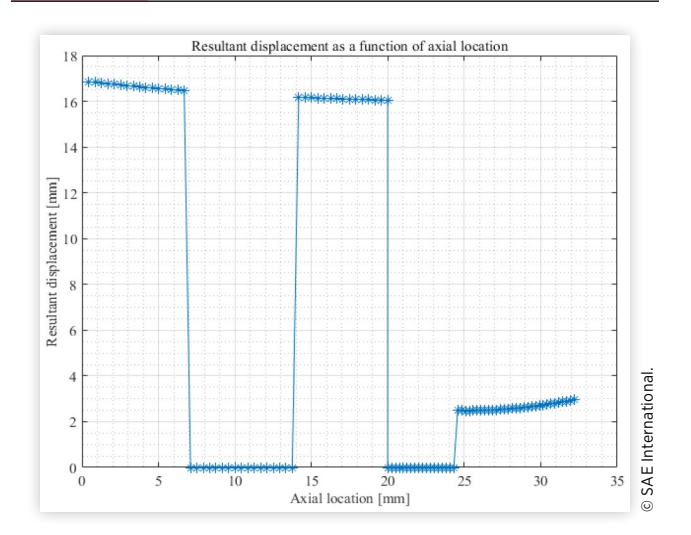
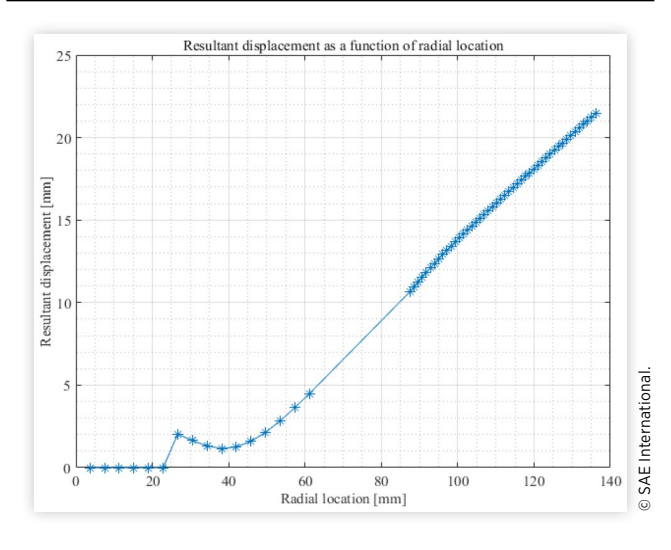


FIGURE 5 Resultant displacement vs. radial location



represent in mm the radial and axial locations on the created paths, and the y-axis in <u>Figures 4</u> and <u>5</u> represents the nodes' displacement in mm at the corresponding locations. While the y-axis in <u>Figures 9</u> and <u>10</u> represents the temperature of each node in the radial and axial direction.

# Effect of Temperature Profile on Thermal Buckling

The critical buckling temperature is defined as the product of the highest nodal temperature and the computed eigenvalue. The eigenvalue determines the lowest acceptable thermal load before buckling occurs. The temperature profile affects the critical buckling temperature and the associated buckling deformation mode which is evident in Table 4. The temperature distributions in the analysis are set as increasing from the hat radius to the outer radius of the rotor following either a linear, sinusoidal, or exponential pattern, meanwhile having the inner and outer radii free to move but constrained at the bolt holes. Figure 6 shows a radially increasing linear temperature profile applied to the brake rotor. Figure 7 shows the first

**TABLE 4** Calculated buckling temperature with obtained eigenvalues

Temperature Profile	Linear	Sinusoidal	Exponential
Eigenvalue	25.637	23.688	38.259
Buckling Temperature [°C]	6409.25	5922	9564.75

© SAE International.

FIGURE 6 Linear temperature profile in the radial direction

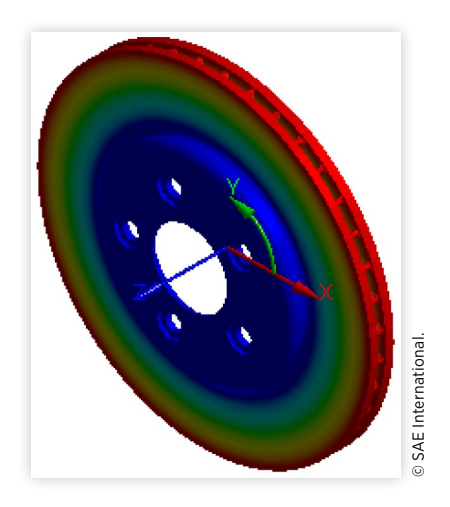
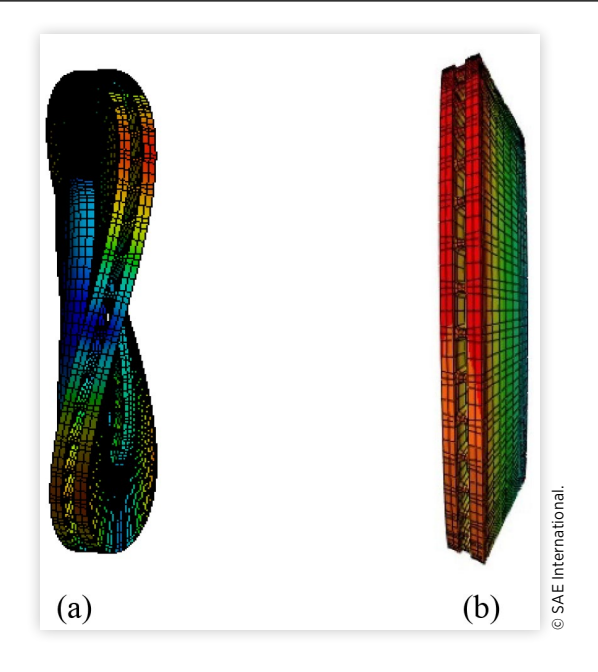


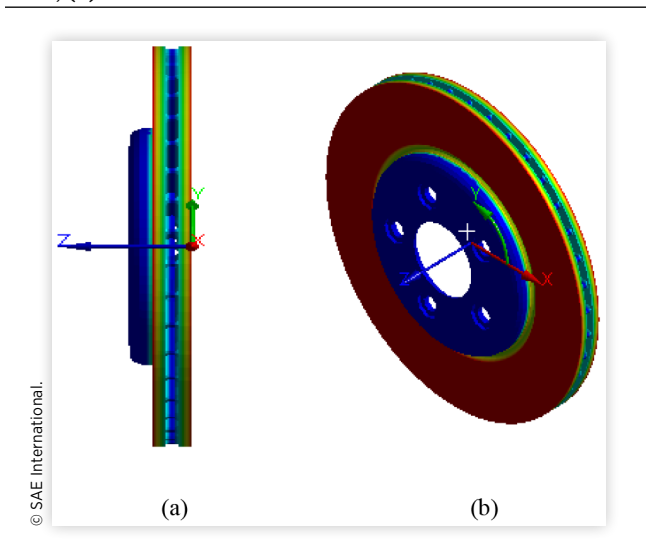
**FIGURE 7** Buckling modes for linear temperature radially distributed: (a) Mode 1 "potato chip mode; (b) Mode 3 "coning mode"



and third buckling modes respectively, which are also known as the potato chip and coning modes because of the resemblance to a potato chip and cone. Figure 8 shows an axially distributed linear temperature. Equations 3, 4, and 5 describe the linear, sinusoidal, and exponential temperature profiles used for the bucking study respectively.

$$228 \times \left(\frac{R - 92}{144 - 92}\right) + 22\tag{3}$$

FIGURE 8 Linear temperature distributed axially: (a) Side View; (b) Iso view



$$228 \times sin(0.0302 \times (R-92)) + 22$$
 (4)

$$\frac{228 \times \left(\exp(0.104 \times (R-92)) - 1\right)}{4.3 \times (144 - 92)} + 22 \tag{5}$$

The equations and constants are chosen such that the temperature difference for each scenario is the same at 228°C across the radius, with a low of 22°C at the hat radius and a high of 250°C at the outer radius. The blue color in the figures indicates the low temperature and the red indicates the high temperature.

The axially distributed temperature is shown to reduce linearly from the outer surface to the midplane of the rotor thickness. The resulting mode 1 eigenvalue, and buckling temperature associated with this axially distributed temperature are 82.256 and 20,564°C respectively. This result shows that a temperature distributed axially has a significant effect on the buckling temperature than a temperature distributed radially.

## Effect of Vibration on Thermal Buckling

Due to the initial assumption shown in Equation 1, the temperature profiles follow the same profiles as the displacement plots shown in Figures 4 and 5. Tables 5 and 6 show the calculated values for k, based on the maximum resultant displacement obtained from the vibration simulation. Figures 9 and 10 are plots of the nodal temperature vs. radial location and of nodal temperature vs. axial location respectively. The maximum and minimum temperatures calculated using Equation 1 are 249.99°C and 23.719°C respectively. Tables 7 and 8 show the resulting eigenvalues and buckling temperatures in the presence of vibration.

A curve fitting technique was utilized to generate an expression for the radial temperature profile varying from the inner radius to the outer radius shown in <u>Figure 9</u> and the axial temperature profile shown in <u>Figure 10</u>. The technique

**TABLE 5** Values of k based on the displacements vs radial location for each rotational velocity

Rotational Velocity [rad/s]	29	63	86
Maximum Displacement (mm)	24.060	22.304	21.468
Value of k	10.391	10.728	11.645

© SAE International

**TABLE 6** Values of k based on the displacements vs axial location for each rotational velocity

Rotational Velocity [rad/s]	29	63	86
Maximum Displacement [mm]	18.888	17.510	16.854
Value of k	13.256	14.278	14.833

© SAE International.

**FIGURE 9** Radial temperature profile associated with 86rad/s rotational velocity

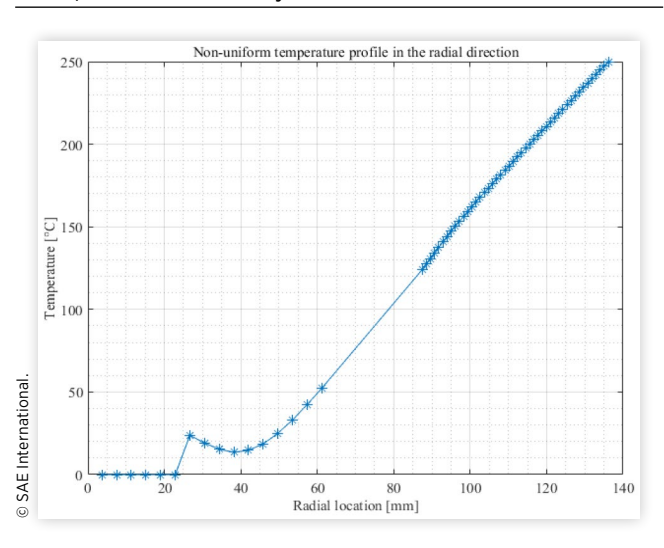


**FIGURE 10** Axial temperature profile associated with 86rad/s rotational velocity

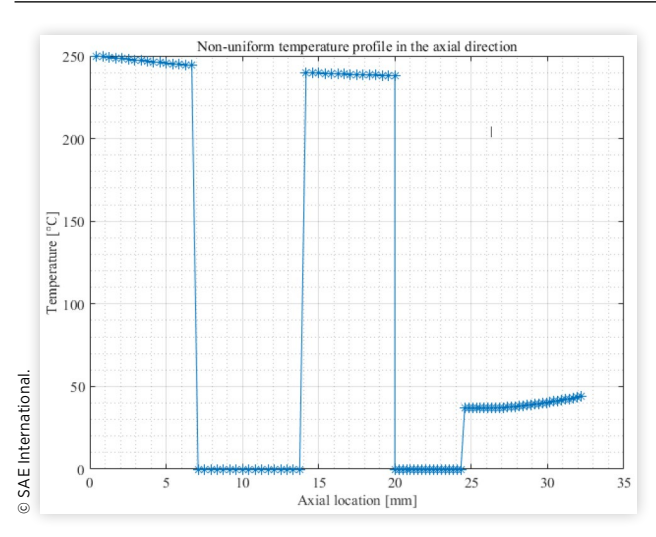


**TABLE 7** The buckling temperature at the studied rotational velocities with a radially distributed temperature

Rotational Velocity [rad/s]	29	63	86
Eigenvalue	38.107	39.857	38.109
Buckling Temperature [°C]	9527.035	9536.875	9527.056

© SAE International.

**TABLE 8** The buckling temperature at the studied rotational velocities with an axially distributed temperature

Rotational Velocity [rad/s]	29	63	86
Eigenvalue	119	119.19	119.2
Buckling Temperature [°C]	29795.137	29798.430	29799.452

© SAE International

determined an eight order polynomial best fits the radial temperature profile in the form shown in <u>Equation 6</u> and a sinusoidal model for the axial temperature profile in the form shown in Equation 7.

$$p_1 x^8 + p_2 x^7 + p_3 x^6 + p_4 x^5 + p_5 x^4 + p_6 x^3 + p_7 x^2 + p_8 x + p_9$$
 (6)

$$a_1 \sin(b_1 + c_1) + a_2 \sin(b_2 + c_2) + \dots + a_8 \sin(b_8 + c_8)$$
 (7)

## Effect of Buckling Mode on Vibration Mode

In a coupling situation, the phenomenon coupled is suspected to influence each other. Therefore, the study of the effect of thermal buckling modes on vibration modes is conducted. The buckling modes obtained thermal buckling simulation with various temperature profiles are used as influencers in the vibration simulation to determine the influence of thermal buckling on vibration. The displacement obtained from the first buckling mode is used as an initial condition in addition to the rotational velocity for the vibration study. The resulting displacement from this vibration simulation is larger because the overall displacement is a concatenation of the initial nodal displacement and the displacement resulting from the rotational velocity.

#### **Future Work**

A more realistic temperature profile for a thermal buckling analysis can be achieved with a transient dynamic analysis with all the brake components included in the analysis. Axial run-out in a brake disc is a type of vibration-induced phenomenon that was not studied in detail in the past. Meanwhile, a more accurate modeling approach can be employed in the future, such as an explicit dynamic simulation to simulate the contact of the brake pads and rotor in the presence of vibrational displacement to better understand how this can affect the heat generation, heat dissipation, wear rate, and the structural integrity of the brake pad and rotor. Vibration in a brake disc can occur in a different

number of ways such as low-frequency vibration that occurs due to non-uniformity caused by "hot spots". The localized hot and cold regions can be hypothesized that they cancel out each other and would not cause thermal buckling. However, in future research, a multistage coupling of thermoelastic instability, vibration, and thermal buckling should be analyzed to investigate the validity of this hypothesis in more depth.

## **Conclusions**

It can be concluded that vibration during braking does not significantly increase the chance of buckling for the ABAQUS benchmark model, the results are highly dependent on the chosen parameters including materials, dimensions, and rotational velocity, and the coupling can be strong in some conditions. This is evident as shown in <u>Tables 7</u> and <u>8</u>- the buckling temperatures are greater than the operating temperatures of 250°C. Vibration modes are affected in the presence of thermal buckling, the displacement present during thermal buckling tends to excite the vibration modes. It is also noted in Tables 7 and 8 that the difference in the buckling temperature is not significant, because the displacements witnessed during vibration at the studied speeds were relatively close. At different speeds other than what was studied in this paper might show a significant difference in the buckling temperatures.

## References

- 1. Bloch, H.P., and Geitner, F.K., *Machinery Failure Analysis* and *Troubleshooting* (Butterworth-Heinemann, 2012).
- Hajnayeb, A., Baghi Abadi, M., and Hosseingholizadeh, A., "An Experimental and Theoretical Study on the Vehicle Brake Judder," SAE Technical Paper 2012-01-1820, 2012, <a href="https://doi.org/10.4271/2012-01-1820">https://doi.org/10.4271/2012-01-1820</a>.
- Meyer, R., "Brake Judder Analysis of the Excitation and Transmission Mechanism within the Coupled System Brake, Chassis and Steering System," SAE Technical Paper 2005-01-3916, 2005, https://doi.org/10.4271/2005-01-3916.
- 4. Prokofévič, T.S., and Gere, J.M., *Theory of Elastic Stability* (Dover Publ, 2009).
- Stibich, P.R., Wu, Y., Zhang, W., Guo, M. et al., "A Technique to Predict Thermal Buckling in Automotive Body Panels by Coupling Heat Transfer and Structural Analysis," SAE Technical Paper <u>2014-01-0943</u>, 2014, <a href="https://doi. org/10.4271/2014-01-0943">https://doi. org/10.4271/2014-01-0943</a>.
- Audebert, N. et al., "Buckling of Automatic Transmission Clutch Plates due to Thermoelastic/Plastic Residual Stresses," *Journal of Thermal Stresses* 21(3):309-326, 1998, doi:10.1080/01495739808956149.
- 7. Ma, C., "Thermal Buckling of Automotive Brake Discs," Dissertation, University of Michigan.

- 8. Palmer, E. et al., "An Optimization Study of a Multiple-Row Pin-Vented Brake Disc to Promote Brake Cooling Using Computational Fluid Dynamics," *Proceedings of the Institution of Mechanical Engineers, Part D: Journal of Automobile Engineering* 223(7):865-875, 2009, doi:10.1243/09544070jauto1053.
- 9. Simulia, I., "ABAQUS/Explicit User's Manual," Version 6.13, Providence, RI, 2017.
- 10. Maluf, O., Angeloni, M., Milan, M., Spinelli, D. et al., "Development of Materials for Automotive Disc Brakes," *Pesquisa Technol Minerva* 2, 2004.
- 11. Belhocine, A., and Bouchetara, M., "Thermal Analysis of a Solid Brake Disc," *Applied Thermal Engineering* 32:59-67, 2012, doi:10.1016/j. applthermaleng.2011.08.029.
- 12. Daws, J.W. et al., "The Impact of Plus-Sized Wheel/Tire Fitment on Vehicle Stability4," *Tire Science and Technology* 35(1):23-40, 2007, doi:10.2346/1.2698541.

#### **Contact Information**

#### Joseph-shaahu Shaahu

PhD student Mechanical & Materials Engineering University of Denver 2155 E Wesley Ave Denver, CO 80208 Joseph-shaahu.shaahu@du.edu

and

#### Yun-Bo Yi, Ph.D.

Professor Mechanical & Materials Engineering University of Denver 2155 E Wesley Ave Denver, CO 80208 Yun-Bo.Yi@du.edu

Phone: 303-871-2228

<sup>© 2020</sup> SAE International. All rights reserved. No part of this publication may be reproduced, stored in a retrieval system, or transmitted, in any form or by any means, electronic, mechanical, photocopying, recording, or otherwise, without the prior written permission of SAE International.